

RESEARCH ARTICLE

A Comprehensive Library of Familial Human Amyotrophic Lateral Sclerosis Induced Pluripotent Stem Cells

Ying Li^{1,2}, Umamahesw Balasubramanian^{1,2}, Devon Cohen^{1,2}, Ping-Wu Zhang^{1,2}, Elizabeth Mosmiller^{1,4}, Rita Sattler^{1,2}, Nicholas J. Maragakis^{1,4}, Jeffrey D. Rothstein^{1,2,3*}

1 Department of Neurology, Johns Hopkins University, School of Medicine, Baltimore, Maryland, 21205, United States of America, **2** Brain Science Institute, Johns Hopkins University, Baltimore, Maryland, 21205, United States of America, **3** Department of Neuroscience, Johns Hopkins University, School of Medicine, Baltimore, Maryland, 21205, United States of America, **4** Ansari ALS Center for Stem Cell and Regeneration Research at Johns Hopkins, Baltimore, Maryland, 21205, United States of America

* jrothstein@jhmi.edu



OPEN ACCESS

Citation: Li Y, Balasubramanian U, Cohen D, Zhang P-W, Mosmiller E, Sattler R, et al. (2015) A Comprehensive Library of Familial Human Amyotrophic Lateral Sclerosis Induced Pluripotent Stem Cells. PLoS ONE 10(3): e0118266. doi:10.1371/journal.pone.0118266

Academic Editor: Huaibin Cai, National Institute of Health, UNITED STATES

Received: December 9, 2014

Accepted: January 12, 2015

Published: March 11, 2015

Copyright: © 2015 Li et al. This is an open access article distributed under the terms of the [Creative Commons Attribution License](https://creativecommons.org/licenses/by/4.0/), which permits unrestricted use, distribution, and reproduction in any medium, provided the original author and source are credited.

Data Availability Statement: All relevant data are within the paper and its Supporting Information files.

Funding: This study was supported by National Institutes of Health (NIH/NINDS; NS069395; 5U24NS078736), P2ALS, Robert Packard Center for ALS Research, Emerald Foundation, Brain Science Institute and Muscular Dystrophy Association (to J. D. R.); the ALS Association (Milton Safenowitz Postdoctoral Fellowship to Y. L.); NIH/NINDS 5U01NS062713, Department of Defense ALSRP, Ansari Center for ALS Cell Therapy and Regeneration Research at Johns Hopkins (to N. J.

Abstract

Amyotrophic lateral sclerosis is a progressive disease characterized by the loss of upper and lower motor neurons, leading to paralysis of voluntary muscles. About 10% of all ALS cases are familial (fALS), among which 15–20% are linked to Cu/Zn superoxide dismutase (SOD1) mutations, usually inherited in an autosomal dominant manner. To date only one FDA approved drug is available which increases survival moderately. Our understanding of ALS disease mechanisms is largely derived from rodent model studies, however due to the differences between rodents and humans, it is necessary to have humanized models for studies of disease pathogenesis as well as drug development. Therefore, we generated a comprehensive library of a total 22 of fALS patient-specific induced pluripotent stem cell (iPSC) lines. These cells were thoroughly characterized before being deposited into the library. The library of cells includes a variety of C9orf72 mutations, *sod1* mutations, FUS, ANG and FIG4 mutations. Certain mutations are represented with more than one line, which allows for studies of variable genetic backgrounds. In addition, these iPSCs can be successfully differentiated to astroglia, a cell type known to play a critical role in ALS disease progression. This library represents a comprehensive resource that can be used for ALS disease modeling and the development of novel therapeutics.

Introduction

Amyotrophic lateral sclerosis (ALS), also known as Lou Gehrig's disease, is a fatal disease characterized by the loss of upper and lower motor neurons, leading to paralysis of voluntary muscles [1]. The mechanisms involved in ALS pathogenesis are largely unknown [2]. About 10% of all cases are inherited, among which about 15–20% are linked to Cu/Zn superoxide dismutase (SOD1) mutations [3] and 40% to C9orf72 mutations [4,5]. Other genes, such as TDP-43,

M.). The funders had no role in study design, data collection and analysis, decision to publish, or preparation of the manuscript.

Competing Interests: The authors have declared that no competing interests exist.

FUS/TLS [6], angiogenin [4,5,7], and very recently Matrin3 [8] have been also found to be linked to familial ALS (fALS). Insights from patient studies have been useful, but limited due to the inaccessibility of tissue from patients except postmortem specimens. While postmortem tissue can only provide end-stage changes, which are not typically suitable for mechanistic studies, other models are indispensable for ALS pathogenesis studies. One of the strategies is to generate rodent models with disease-specific mutations, such as different human SOD1 (hSOD1) mutations and TDP43 mutations. Some animals develop signs and pathological changes resembling those in patients [9–11], which are enormously valuable in disease study, however, not all transgenic mice with hSOD1 mutations develop the disease [12].

To date, only one drug, riluzole, is FDA approved for delaying disease progression for ALS patients with only modest efficacy in increasing survival [13]. The vast majority of novel therapeutics for ALS has advanced to the clinic following studies in rodent transgenic models of the mutant SOD1 form of ALS. Unfortunately, most drugs have failed Phase 2 and 3 trials, which can be due to several reasons, including (1) poor human and mouse trial design; (2) the mutant SOD1 mouse model may not be predictive of the pathophysiological process in the more common sporadic form(s) of ALS; (3) lack of proper pharmacokinetics, (4) lack of pharmacodynamic markers in human studies; (5) lack of evidence for target engagement by candidate drugs in human studies. In summary, it has been a growing concern that preclinical rodent models are not sufficiently predictive of complex neurodegenerative diseases [14].

Fortunately, significant progress in human induced pluripotent stem cell (iPSC) research provides a novel valuable tool for ALS research. Soon after the first reports on human iPSC generation [15,16], neurological disease specific iPSCs had been successfully generated from patients' somatic cells [17–23], including several for ALS [18]. Remarkably, these cells can be differentiated to the type of cells which are critical for disease development, such as motor neurons from ALS-iPSCs [18,24–26], and they have been successfully used in disease modeling in neurological diseases like ALS, spinal muscular atrophy and familial dysautonomia [20,21,27]. ALS rodent studies have provided strong evidence that ALS is also a non-cell autonomous disease [28–32] as oligodendroglia may play a significant role in disease initiation and both astroglia and microglia play a role in disease progression. Further co-cultures of rodent glial cells, human fetal astrocytes overexpressing mutant hSOD1, or adult fALS and sALS astrocytes with motor neurons derived from human embryonic stem cells (hESCs) also showed non-cell autonomous effects on human motor neurons [27,33,34]. These studies together not only strongly suggest that non-cell autonomous mechanisms are involved in human ALS pathogenesis, but also provide evidence that patient specific iPSCs and hESCs are valuable for studying the disease. In addition, very recent studies with ALS C9orf72 iPSC cell lines provide compelling evidence that the cells can have utility that exceeds prior disease models. These characteristics include: replication of actual human brain pathology, mimicking gene transcriptional changes seen in human disease, elucidating pathophysiological pathways and a cell culture platform for human drug screening and drug efficacy biomarkers [35][36].

Here we report that we generated a library of familial ALS patient-specific iPSCs (fALS-iPSCs) carrying a large variety of ALS mutations. These fALS-iPSCs can be differentiated to astroglia, a critical cell type that plays a role in ALS progression. In order to be widely useful, this “library” is based on the more common different ALS mutations, including SOD1 and FUS, and several lines of the same mutation are collected from different families. The fALS-iPSCs and their parental fibroblasts were generated to be publicly available to academic and commercial entities alike. The fibroblast lines have been reported separately [37]. We believe this widely available fALS-iPSC library will provide a great tool to study ALS pathophysiology, for biomarker development and for the preclinical development of novel therapies.

Materials and Methods

Patient Consent

The use of human tissues and associated demographic information was approved by the Johns Hopkins University Institutional Review Board and Ethics Committee (HIPAA Form 5 Exemption, Application #11-02-10-01RD). All skin biopsies were collected following written informed consent from the donor. The informed consent was approved by the Johns Hopkins University Institutional Review Board and Ethics Committee of Johns Hopkins Hospital (IRB protocol: NA-00021979). The consent allowed for use by all parties, commercial and academic, for research purposes only but not for human therapy.

ALS-iPSC generation and characterization

The Sox2, Oct4, Klf4 and c-Myc encoding vectors were transduced into ALS-fibroblasts by using retrovirus based delivery. All iPSC cell lines were created and initially characterized with an NIH-sponsored commercial agreement with iPierian (USA). Promising colonies were picked and evaluated for the expression of multiple pluripotent markers by quantitative PCR (qPCR) and/or immunocytochemistry. Their in vitro pluripotency was further determined by three germ layer differentiation via embryoid body formation. The transgene expression was determined by qPCR. Individual PCR reactions were normalized against *GAPDH* and plotted relative to the expression level in the control H9 and/or H7 Human ES cells. All iPSC cell lines and fibroblasts were deposited with Coriell (<http://www.coriell.org>) for widespread public distribution.

iPSC culture and differentiation

The iPSCs were maintained in mTeSR1 (StemCell Technology) and passed once a week using dispase (StemCell Technology) following the manufacturer's instructions. Partially differentiated colonies were removed manually before differentiation analyses. The iPSCs were differentiated to neuroprogenitor cells (NPCs) via embryoid body (EB) formation by following the methods described previously [38]. To increase the efficiency of NPC differentiation, SMAD pathway was inhibited during neural induction, and the NPCs were then further differentiated to astrocyte by following the methods described previously [39,40].

Immunocytochemistry

The cells were fixed with 4% paraformaldehyde at room temperature (RT) for 10min, and then permeabilized with 0.1% Triton X-100 in PBS at RT for another 10min. After incubation with 10% donkey serum or 3% BSA for 20min at room temperature, the primary antibody was applied and incubated at RT for 1hr and Alexa Fluor 488 or 555 labeled secondary antibody for another hour. Nuclei were stained with DAPI. Images were randomly taken using a Nikon microscope with SPOT camera. Primary antibodies used in the study are listed in [S1 Table](#).

Statistical analysis

Statistic analysis was performed by Prism (GraphPad Software). Student's t test was used for the percentage of rosette positive colony comparison between control and SOD1 groups. One-way ANOVA with Tukey's post analysis was carried out to compare maker expression at different time points. $P < 0.05$ was considered significant. Data are summarized from more than three independent experiments and shown as mean \pm SEM.

Results

Generation and characterization of fALS-iPSCs

The human (healthy and ALS subject) dermal fibroblasts were collected through a nationwide National Institutes of Health supported collaboration (Johns Hopkins University School of Medicine, Massachusetts General Hospital and Emory University ALS Center). The fibroblast cultures were established at Johns Hopkins School of Medicine for iPSC generation. A total of four healthy control iPSC lines, twenty-two fALS-iPSC lines and two sporadic ALS-iPSC lines with c9of72 repeat mutation were generated (summarized in [Table 1](#)). These mutations cover twelve different *sod1* mutations, three *FUS* mutations, one angiogenin (*ANG*) and one *FIG4* mutation. All iPSCs have been generated by using Sox2, Oct4, Klf4 and c-Myc factors delivered by retroviruses with a programming efficiency of ~0.1%. Putative iPSCs underwent a validation profile that included: 1) morphological analysis, compact colonies with clear boundary and are comprised of cells with big nucleus and large nucleoli and scant cytoplasm ([Fig. 1A](#)); 2) pluripotent gene expression by quantitative PCR, including *CDH1*, *Dnmt3b*, *FoxD3*, *GDF3*, *Lefty1/2*, *LIN28*, *Nanog*, *Nodal*, *Sall4*, *TDGF1*, *TDGF1&3*, *TERT*, *Zfp42* and *ZNF206*, and their expression were comparable with hESCs (H9 and/or H7) ([Fig. 1E](#) and [S1 Fig.](#)); 3) pluripotent marker expression by immunocytochemistry, such as Tra1–81 and SSEA4 ([Fig. 1A](#)), Tra1–60 and SSEA3 (not shown), 3) silencing of transgenes and upregulation of endogenous Sox2, Oct4, Klf4 and Myc ([Fig. 1B](#) and [S1 Fig.](#)); 4) in vitro differentiation to three germ layers via EB formation ([Fig. 1C](#) and [S2 Fig.](#)). The expression of ectoderm cell markers such as neuron marker *Tuj1*, mesoderm cell markers such as smooth muscle antigen (aSMA) or desmin, and endoderm cell markers alpha fetoprotein (AFP) or forkhead box protein A2 (*FoxA2*), were evaluated by immunocytochemistry; 5) normal karyotypes ([Fig. 1D](#) and [S3 Fig.](#)). Only cells meeting all these criteria were deposited into the library. The cells were maintained in mTeSR1 medium.

Differentiation of fALS-iPSCs to NPCs

ALS-iPSCs have been successfully differentiated to motor neurons [[18](#)], but there were no detailed reports whether the presence of mutant SOD1 interferes with neural progenitor differentiation. In the differentiation studies, we focused on iPSC lines with *sod1* mutations (line 001, 002, 003, 008, and 013), and controls (line 005, 006 and 018). We first followed the well-established method to differentiate the cells to NPCs via EB formation. Both control and SOD1-iPSC generated rosettes structure after about ten days of induction and developed to neural tube like rosettes at around 12–14 days. The cells in the neural tube like structures expressed NPC marker *Pax6* and *Sox1* ([Fig. 2A](#)), and no significant differentiation differences were seen between control and SOD1-iPSCs (control $67.3 \pm 2.4\%$ vs $65.6 \pm 1.2\%$, [Fig. 2B](#)), suggesting that the presence of mutant SOD1 had no obvious effects on neural induction. As inhibition of SMAD pathway can increase the efficiency of neural induction [[39,40](#)], we next applied SB431542 and LDN193189 for one week for neutralization following the protocol developed by our ALS consortium [[40](#)]. Both control and SOD1-iPSCs were efficiently differentiated to NPCs expressing *Pax6* (control $89.3 \pm 4.2\%$ vs SOD1 $83.1 \pm 4.5\%$, $P > 0.05$), *Sox1* (control $77.2 \pm 3.7\%$ vs SOD1 $80.8 \pm 3\%$, $P > 0.05$) and *Sox2* (control $76.1 \pm 5.6\%$ vs SOD1 $83.9 \pm 2.1\%$, $P > 0.05$) at week 2 of induction ([Fig. 2C](#)). The expression of *Pax6* dramatically decreased at week 4 (control $21 \pm 5\%$ vs SOD1 $27.6 \pm 8.2\%$, $P > 0.05$), and *Sox1* (control $65.4 \pm 4.1\%$ vs SOD1 $67.7 \pm 11.6\%$ at week 4, $P > 0.05$; control $54.5 \pm 15.3\%$ vs SOD1 $56.2 \pm 3.3\%$ at week 5, $P > 0.05$) and *sox2* (control $63.7 \pm 4.9\%$ vs SOD1 $59.9 \pm 1.4\%$, $P > 0.05$) gradually decreased at week 4–5 ([Fig. 2D](#)) when the medium was changed for further astroglia differentiation. No significant differences in

Table 1. fALS-iPSC lines.

ID	Gene	Mutation	Age at biopsy (year)	Disease length at Biopsy (month)	Clinical site at onset	Gender	Race
Control							
005	Control	NA	66	NA	NA	M	W
006	Control	NA	68	NA	NA	M	W
010	Control	NA	50	NA	NA	F	W
018	Control	NA	55	NA	NA	F	W
Familial ALS							
002	SOD1	A4V	57	NA	NA	F	W
007	SOD1	A4V	40	NA	NA	F	W
008	SOD1	A4V	45	NA	NA	F	W
013	SOD1	A4V	63	10	spinal	F	W
021	SOD1	C38G	47	34	spinal	M	A
004	SOD1	D90A	50	96	spinal	F	W
028	SOD1	D90A	68	83	spinal	F	W
017	SOD1	D91A	56	103	spinal	M	W
026	SOD1	E100G	41	47	spinal	M	W
024	SOD1	E49K	49	36	spinal	F	W
033	SOD1	G86R	77	NA	NA	M	W
003	SOD1	I112T	44	NA	NA	F	W
016	SOD1	I113T	53	60	spinal	M	W
015	SOD1	L144P	51	30	spinal	M	W
001	SOD1	N139K	46	46	spinal	M	AA
009	SOD1	V148G	54	6	spinal	M	W
027	ANG	ND	55	10	bulbar	M	W
014	FIG4	ND	67	12	bulbar	F	W
025	FUS	H517Q	50	96	spinal	F	AA
031	FUS	T198C	57	23	bulbar	M	W
023	FUS	G522A	37	13	spinal	M	W
034	VCP	ND	64	132	spinal	F	W
C9orf72							
033	C9orf72	>800 repeats	62	43	Spinal	M	W
034M	C9orf72	>800 repeats	65	33	Bulbar	F	W

Note: NA, not applicable/not known; ND, not determined; M, male; F, female; W, white; AA, African American.

each marker expression between control and SOD1-iPSCs were observed at each time point. Similar differentiation was seen with the C9orf72 iPSC cell lines (non shown). Notably for the C9orf72 iPSC cell lines previously we demonstrated that the expansion mutation was maintained [35].

Differentiation of fALS-iPSCs to astroglia

To test whether the iPSC cells in this library can be efficiently differentiated to astroglia and whether these allelic mutations could alter that process, we followed the protocol developed by our ALS consortium [40]. We treated the NPCs, which were induced by inhibition of SMAD pathway, with fetal bovine serum (FBS) to induce astrogliogenesis. The NPCs changed their morphology dramatically to a more flattened shape after about two weeks. Both control and SOD1-iPSCs expressed the astroglia progenitor marker CD44 [41] as early as 5 weeks in a low

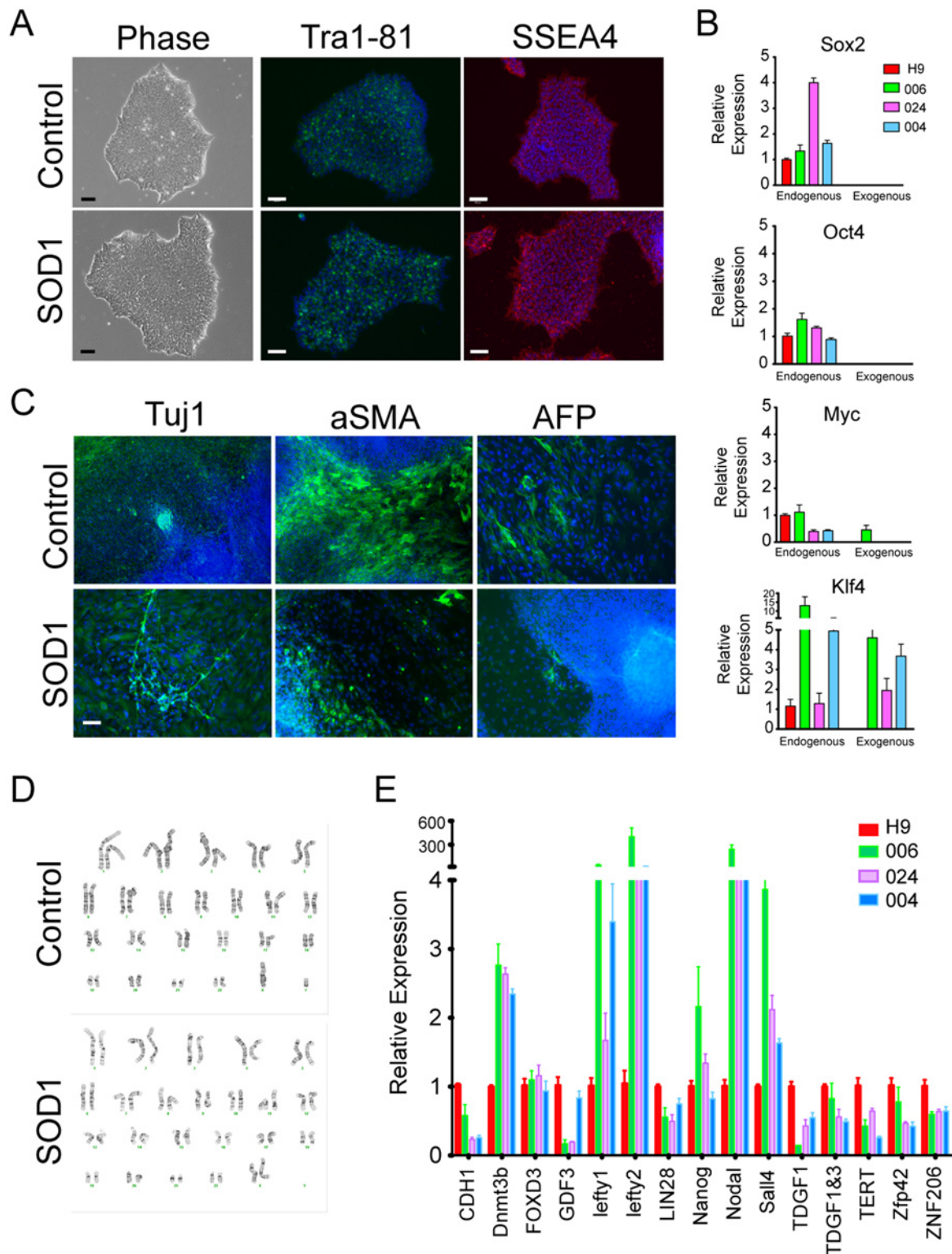


Fig 1. Characterization of fALS-iPSCs. (A) Representative pictures of control- (006) and SOD1-iPSC (002) morphology and their expression of Tra1-81 (green) and SSEA4 (red). Nuclei were stained with DAPI (blue). Size bar: 100µm. (B) Representative qPCR evaluation of endogenous and transgene expression by control- (006) and SOD1-iPSCs (004 and 024). (C) Representative pictures show both control (006) and SOD1-iPSCs (024) generated cells representing the three embryonic germ layers (Tuj1, aSMA and AFP, all in green). Nuclei were stained with DAPI (blue). Size bar: 100µm. (D) Representative karyotypes of control- (006) and SOD1-iPSCs (024). (E) Representative qPCR results of pluripotent marker expression by control (006) and SOD1-iPSC (004 and 024) lines.

doi:10.1371/journal.pone.0118266.g001

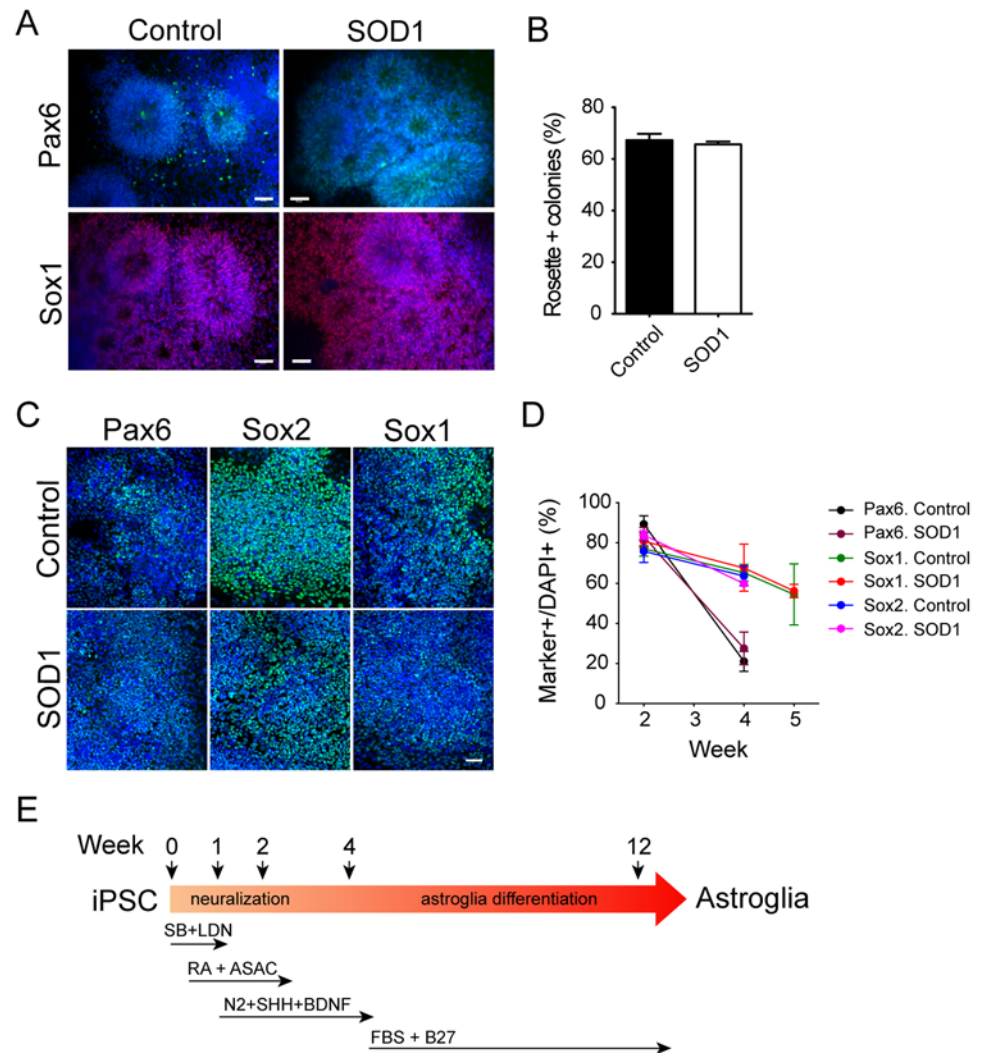


Fig 2. Differentiation of SOD1-iPSCs to NPCs. (A, B) NPCs were generated via EB formation. (A) Rosettes and neural tube structures were formed and the cells expressed Pax6 and Sox1. Representative pictures were taken from 006 control and 002 SOD1 lines. Nuclei were stained with DAPI. (B) Quantification of colonies with rosette structures. (C, D) NPCs were induced by inhibition of SMAD pathway. Most cells expressed Pax6, Sox2 and Sox1 at week 2. Nuclei were stained with DAPI. (D) Dynamic examination of Pax6, Sox1 and Sox2 expression by NPCs after 2–5 week. (E) Time line of neural induction by the inhibition of SMAD pathway and astrocyte differentiation. Size bar, 50µm.

doi:10.1371/journal.pone.0118266.g002

percentage of cells (control $17.8 \pm 6.3\%$ vs SOD1 $8.3 \pm 3.7\%$) and rapidly increased over the next two weeks (control $76.2 \pm 5\%$ vs SOD1 $65.8 \pm 5.4\%$ at week 7) followed by steady increases (from week 9 to week 11, control $83.6 \pm 5.4\%$ to $92.6 \pm 3.7\%$ vs SOD1 $78.4 \pm 7.3\%$ to $97.9 \pm 0.9\%$) (Fig. 3C). GFAP expression was observed as early as week 4, but the cells were bipolar and had long processes, which we previously interpreted as radial glial and not bona fide astroglia [40]. Cells with flattened morphology started to express GFAP as early as week 5 but at very low percentage (control $3.4 \pm 3.4\%$ vs SOD1 $0.4 \pm 0.1\%$). In the next four weeks GFAP expression increased rapidly (from week 7 to 9, control $9 \pm 2.9\%$ to $37.2 \pm 4.6\%$ vs SOD1 $4.5 \pm 2.6\%$ to $50 \pm 7.3\%$), and then increased steadily (week 12–13, control $55.8 \pm 7.9\%$ vs SOD1 $63.8 \pm 7.8\%$) (Fig. 3B). After 7 weeks, most cells showed flattened morphology, and most of them expressed

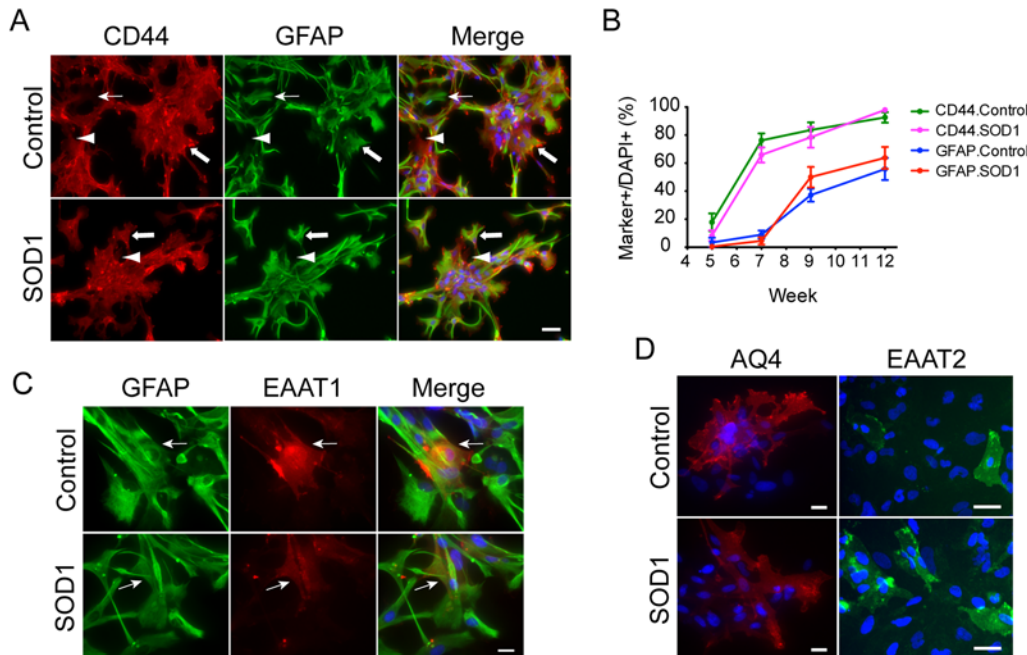


Fig 3. Differentiation of SOD1-iPSCs to astroglia. Representative pictures of control (006) and SOD1-iPSC (008) derived astrocyte after 15-week differentiation showing astroglial marker expression. (A) CD44 (red) and GFAP (green) expression by differentiated cells. Thin arrows indicate GFAP+ only cells. Arrowheads indicate CD44+ only cells. Thick arrows indicate CD44+/GFAP+ cells. (B) Quantification of CD44+ and GFAP+ cells at different time points. (C) EAAT1 (red) expression by GFAP+ (green) astrocytes. Arrows indicate double positive cells. (D) Aquaporin 4 (AQ4, red) and EAAT2 (green) expression. Nuclei were stained with DAPI (blue). Size bar, 20µm.

doi:10.1371/journal.pone.0118266.g003

CD44. CD44+/GFAP-, CD44+/GFAP+ and CD44-/GFAP+ cells were easily observed after week 9, suggesting astroglia progenitors differentiated toward astroglia steadily, but slowly. After 13 weeks, a very small percentage (less than 10%) of cells expressed more mature physiologically and synaptically relevant astroglial markers, EAAT2 (known as GLT1 in rodents), EAAT1 (known as GLAST in rodents), and aquaporin 4 (Fig. 3A), suggesting that the cells were developing appropriate astroglial functional properties. We did not observe significant differences in these maturation markers between control and mutant SOD1 expressing cells at any analyzed time points. The small percentages of cells expressing the mature astroglial marker EAAT2, for example, suggests that, while these cells have mature features of astroglia, they likely remain immature astrocytes at the in vitro time points studied, as suggested by the previous study in a very small number of iPS lines [40].

During the differentiation, we also observed that most of the differentiating cells started to express S100beta and vimentin as early as week 4–5 and reached peak (near 100%) at week 5–6 (not shown). We further examined the cells for any evidence of mutation altering biology. None of the GFAP+ astroglia with SOD1 mutations had evidence of aberrant morphology compared to the control cells. In addition, no evidence for intracellular, either cytoplasmic or nuclear, inclusions with ubiquitin immunoreactivity has been seen (not shown).

Discussion

In 2009, through the American Recovery and Reinvestment Act (ARRA), the National Institutes of Health (NINDS) funded three consortia to develop well-characterized and publicly available iPSCs from familial forms of ALS, Parkinson’s disease (PD) and Huntington’s disease (HD). As a member of this consortium, we were tasked with generating a comprehensive

library of fALS-iPSCs, which includes 22 fALS-iPSC and 4 control lines. This consortium was assembled to collect fALS biopsies and fibroblasts, including relevant clinical information, generating initial iPSC lines, employing a commercial collaborator (iPierian) specialized in rapid reliable development of iPSC lines, and validating their basal biology to differentiate into astroglia and motor neurons. In this report we outline this large collection of diverse fALS-iPSC lines and their reliable differentiation to astroglia. Although sporadic ALS iPSC cell lines could be useful as well, early review of the program provided support for only the generation of cell lines from available fALS patients. Subsequently, our labs have collected over 100 fibroblast lines from sporadic ALS as well (unpublished). Most recently, we generated several c9orf72 ALS/FTD iPSC cell lines from sporadic ALS patients (see above) [42].

iPSCs can be generated from different tissue resources [43–45] by using virus-based delivery of transcription factors [16,46–48], direct delivery of DNA [49–52] or modified mRNA transcripts [53], small molecules or proteins [54]. The cells in the present library have been generated by using Yamanaka's four factors, which was the more mature methodology when the library was being generated and gave better reprogramming efficiency. Recently, other approaches have been employed focused on generating "print free" cell lines (without exogenous gene insertion or retention in the chromosome) and these approaches either suffer from poor efficiency or are costly and time-consuming. As cells generated by different laboratories may have their laboratory-specific molecular and/or genetic "finger print" [55], it could prove difficult to make comparisons between analyses using the cells generated from different resources. All the ALS-iPSCs in this library have been generated in collaboration with iPierian using the same reprogramming methodology, chosen using the same quantitative control, and cultured under the same conditions, which provided maximum control of cell qualities.

We were able to successfully differentiate fALS-iPSCs with different mutant *sod1* primarily into rudimentary GFAP expressing-astroglia and some biologically relevant mature astroglia expressing EAAT1, EAAT2 or aquaporin 4. In the previous report, hESC and healthy human iPSC lines were differentiated to functional astroglia [40]. By using the same protocol, we observed comparable efficiency of NPC and astroglia differentiation of the fALS-iPSCs from this library in terms of the expression of NPC marker Pax6, astroglia progenitor markers CD44 and mature astroglia markers EAAT2, EAAT1 when induced by low percentage of FBS. Therefore, it is very possible the iPSCs in this library can be differentiated to mature functional astroglia by treating with FGF1 or FGF2 as shown in the previous study. However, whether the presence of mutant SOD1, or other ALS mutations, would interfere with astroglia maturation needs further study.

The astroglia derived from this fALS-iPSC library represent the natural disease in terms of allelic copies of the mutant gene, which would provide a faithful model to study cell-cell interactions responsible for disease pathophysiology in ALS and astroglia pathophysiology. From the mutations we tested, there was no gross evidence of aberrant cellular morphology or intracellular inclusions under basal conditions. It is possible that the majority of the cells were immature astroglia, or the cells were not purified or enriched, or extrinsic signals (such as from neurons) are necessary. In vivo studies from both human and mice showed there is dramatic dysregulation of EAAT2 expression in disease and EAAT2 expression is tightly coupled to the presence of neurons [56], future studies could examine the dysregulation of the human iPSC derived astroglia in human neuron-astroglia co-cultures.

In addition to its application in disease modeling, the fALS-iPS derived cells offer a valuable tool for screening and validating CNS compounds. Candidate compounds for treating CNS defects fail in clinical trials in over 90% of cases due to poor targeting, lack of efficacy, and unacceptable side effects [57]. Recent studies using ALS motor neurons derived from iPSCs with mutant TDP43 or SOD1 were successfully used in drug screening [24,58], supporting the use

of iPSC cell culture platforms for drug discovery efforts. Similarly, we have used ALS iPSC neurons derived from C9orf72 mutant patients to successfully generate and validate antisense oligonucleotide candidate therapies [42]. The present library covers 12 *sod1* mutations of the known >105 *sod1* mutations [59], including A4V mutation, the most prevalent mutation in the US which causes rapidly progressing ALS, and D90A mutation that is correlated with slowly progressing ALS. These different mutations show different enzyme activities and/or thermal stabilities. Importantly, there is more than one line available from certain mutations, such as A4V and D90A. Given that these cells were from different families, this could provide important insights into the variability of background genetics, which can influence the properties of the lines and their utility for drug screening. Therefore, this library provides a very valuable resource for drug screening, to test drug toxicity and efficacy among subpopulations [60] as so called “in vitro clinical trial” [61].

During astroglia differentiation, most cells expressed markers of astroglial progenitor fate compared to GFAP and mature astroglial markers. The generation and maturation of iPSC derived-astroglia takes a long time in vitro, which is consistent with human embryonic astroglial development. However, this lengthy time to differentiate provides a platform to screen drugs which may facilitate astroglia development and maturation. For example, as EAAT2 expression is downregulated in ALS [62], maintenance and up-regulation of EAAT2 expression in astrocytes promotes motor neuron survival and prolongs disease duration [63,64]. Screening and validating drugs for EAAT2 expression using ALS-iPSC derived astroglia can potentially provide a therapy for ALS patients.

Supporting Information

S1 Fig. qPCR analysis of pluripotent stem cell marker and transgene expression by fALS-iPSC cells. TaqMan assay was used to determine gene expression. The log ratio is the difference in Ct between gene of interest and the housekeeping gene GAPDH.

(PDF)

S2 Fig. In vitro differentiation potential of fALS-iPSC cells. Embryoid Body culture was used to examine the differentiation potential of the iPSC lines. These aggregates are allowed to grow for several days and then assessed by antibody staining for their ability to differentiate into cell types representing three germ layers.

(PDF)

S3 Fig. Karyotypes of fALS-iPSC cells. The iPSC cells were analyzed between passage number 4 to 10 (P4–P10). Line 010 showed balanced translocation due to reciprocal exchange between the long-arm of chromosome 1 and the short-arm of chromosome 17.

(PDF)

S1 Table. Antibodies used in the study.

(DOCX)

Acknowledgments

We thank the patients and their families for agreeing to participate in this study. We thank Christopher E. Henderson, and Kevin C. Eggen for collaborative discussions and input regarding ALS iPSC cell lines, M. Cudkowicz and M. Benetar for collecting patient biopsy samples and clinical histories, and Cassandra Obie for culturing fibroblasts from skin biopsies.

Author Contributions

Conceived and designed the experiments: YL JDR. Performed the experiments: YL DC. Analyzed the data: YL JDR. Contributed reagents/materials/analysis tools: EM PWZ. Wrote the paper: YL NJM RS JDR. Technical support: UB.

References

1. Mulder DW (1982) Clinical limits of amyotrophic lateral sclerosis. *Adv Neurol* 36: 15–22. PMID: [7180681](#)
2. Rothstein JD (2009) Current hypotheses for the underlying biology of amyotrophic lateral sclerosis. *Ann Neurol* 65 Suppl 1: S3–9. doi: [10.1002/ana.21543](#) PMID: [19191304](#)
3. Pasinelli P, Brown RH (2006) Molecular biology of amyotrophic lateral sclerosis: insights from genetics. *Nat Rev Neurosci* 7: 710–723. PMID: [16924260](#)
4. DeJesus-Hernandez M, Mackenzie IR, Boeve BF, Boxer AL, Baker M, et al. (2011) Expanded GGGGCC hexanucleotide repeat in noncoding region of C9ORF72 causes chromosome 9p-linked FTD and ALS. *Neuron* 72: 245–256. doi: [10.1016/j.neuron.2011.09.011](#) PMID: [21944778](#)
5. Renton AE, Majounie E, Waite A, Simon-Sanchez J, Rollinson S, et al. (2011) A hexanucleotide repeat expansion in C9ORF72 is the cause of chromosome 9p21-linked ALS-FTD. *Neuron* 72: 257–268. doi: [10.1016/j.neuron.2011.09.010](#) PMID: [21944779](#)
6. Da Cruz S, Cleveland DW (2011) Understanding the role of TDP-43 and FUS/TLS in ALS and beyond. *Curr Opin Neurobiol* 21: 904–919. doi: [10.1016/j.conb.2011.05.029](#) PMID: [21813273](#)
7. Majounie E, Renton AE, Mok K, Doppler EG, Waite A, et al. (2012) Frequency of the C9orf72 hexanucleotide repeat expansion in patients with amyotrophic lateral sclerosis and frontotemporal dementia: a cross-sectional study. *Lancet Neurol* 11: 323–330. doi: [10.1016/S1474-4422\(12\)70043-1](#) PMID: [22406228](#)
8. Johnson JO, Piro EP, Boehringer A, Chia R, Feit H, et al. (2014) Mutations in the Matrin 3 gene cause familial amyotrophic lateral sclerosis. *Nat Neurosci* 17: 664–666. doi: [10.1038/nn.3688](#) PMID: [24686783](#)
9. Gurney ME, Pu H, Chiu AY, Dal Canto MC, Polchow CY, et al. (1994) Motor neuron degeneration in mice that express a human Cu,Zn superoxide dismutase mutation. *Science* 264: 1772–1775. PMID: [8209258](#)
10. Wong PC, Pardo CA, Borchelt DR, Lee MK, Copeland NG, et al. (1995) An adverse property of a familial ALS-linked SOD1 mutation causes motor neuron disease characterized by vacuolar degeneration of mitochondria. *Neuron* 14: 1105–1116. PMID: [7605627](#)
11. Rosen DR, Siddique T, Patterson D, Figlewicz DA, Sapp P, et al. (1993) Mutations in Cu/Zn superoxide dismutase gene are associated with familial amyotrophic lateral sclerosis. *Nature* 362: 59–62. PMID: [8446170](#)
12. Deng HX, Shi Y, Furukawa Y, Zhai H, Fu R, et al. (2006) Conversion to the amyotrophic lateral sclerosis phenotype is associated with intermolecular linked insoluble aggregates of SOD1 in mitochondria. *Proc Natl Acad Sci U S A* 103: 7142–7147. PMID: [16636275](#)
13. Cheah BC, Vucic S, Krishnan AV, Kiernan MC (2010) Riluzole, neuroprotection and amyotrophic lateral sclerosis. *Curr Med Chem* 17: 1942–1199. PMID: [20377511](#)
14. Benatar M (2007) Lost in translation: treatment trials in the SOD1 mouse and in human ALS. *Neurobiol Dis* 26: 1–13. PMID: [17300945](#)
15. Takahashi K, Tanabe K, Ohnuki M, Narita M, Ichisaka T, et al. (2007) Induction of pluripotent stem cells from adult human fibroblasts by defined factors. *Cell* 131: 861–872. PMID: [18035408](#)
16. Yu J, Vodyanik MA, Smuga-Otto K, Antosiewicz-Bourget J, Frane JL, et al. (2007) Induced pluripotent stem cell lines derived from human somatic cells. *Science* 318: 1917–1920. PMID: [18029452](#)
17. Park IH, Arora N, Huo H, Maherali N, Ahfeldt T, et al. (2008) Disease-specific induced pluripotent stem cells. *Cell* 134: 877–886. doi: [10.1016/j.cell.2008.07.041](#) PMID: [18691744](#)
18. Dimos JT, Rodolfa KT, Niakan KK, Weisenthal LM, Mitsumoto H, et al. (2008) Induced pluripotent stem cells generated from patients with ALS can be differentiated into motor neurons. *Science* 321: 1218–1221. doi: [10.1126/science.1158799](#) PMID: [18669821](#)
19. Soldner F, Hockemeyer D, Beard C, Gao Q, Bell GW, et al. (2009) Parkinson's disease patient-derived induced pluripotent stem cells free of viral reprogramming factors. *Cell* 136: 964–977. doi: [10.1016/j.cell.2009.02.013](#) PMID: [19269371](#)

20. Ebert AD, Yu J, Rose FF Jr, Mattis VB, Lorson CL, et al. (2009) Induced pluripotent stem cells from a spinal muscular atrophy patient. *Nature* 457: 277–280. doi: [10.1038/nature07677](https://doi.org/10.1038/nature07677) PMID: [19098894](https://pubmed.ncbi.nlm.nih.gov/19098894/)
21. Lee G, Papapetrou EP, Kim H, Chambers SM, Tomishima MJ, et al. (2009) Modelling pathogenesis and treatment of familial dysautonomia using patient-specific iPSCs. *Nature* 461: 402–406. doi: [10.1038/nature08320](https://doi.org/10.1038/nature08320) PMID: [19693009](https://pubmed.ncbi.nlm.nih.gov/19693009/)
22. Hotta A, Cheung AY, Farra N, Vijayaragavan K, Seguin CA, et al. (2009) Isolation of human iPSC cells using EOS lentiviral vectors to select for pluripotency. *Nat Methods* 6: 370–376. doi: [10.1038/nmeth.1325](https://doi.org/10.1038/nmeth.1325) PMID: [19404254](https://pubmed.ncbi.nlm.nih.gov/19404254/)
23. Di Domenico AI, Christodoulou I, Pells SC, McWhir J, Thomson AJ (2008) Sequential genetic modification of the hprt locus in human ESCs combining gene targeting and recombinase-mediated cassette exchange. *Cloning Stem Cells* 10: 217–230. doi: [10.1089/clo.2008.0016](https://doi.org/10.1089/clo.2008.0016) PMID: [18386992](https://pubmed.ncbi.nlm.nih.gov/18386992/)
24. Egawa N, Kitaoka S, Tsukita K, Naitoh M, Takahashi K, et al. (2012) Drug Screening for ALS Using Patient-Specific Induced Pluripotent Stem Cells. *Sci Transl Med* 4: 145ra104. doi: [10.1126/scitranslmed.3004052](https://doi.org/10.1126/scitranslmed.3004052) PMID: [22855461](https://pubmed.ncbi.nlm.nih.gov/22855461/)
25. Chen H, Qian K, Du Z, Cao J, Petersen A, et al. (2014) Modeling ALS with iPSCs Reveals that Mutant SOD1 Misregulates Neurofilament Balance in Motor Neurons. *Cell Stem Cell* 14: 796–809. doi: [10.1016/j.stem.2014.02.004](https://doi.org/10.1016/j.stem.2014.02.004) PMID: [24704493](https://pubmed.ncbi.nlm.nih.gov/24704493/)
26. Kiskinis E, Sandoe J, Williams LA, Boulting GL, Moccia R, et al. (2014) Pathways Disrupted in Human ALS Motor Neurons Identified through Genetic Correction of Mutant SOD1. *Cell Stem Cell* 14: 781–795. doi: [10.1016/j.stem.2014.03.004](https://doi.org/10.1016/j.stem.2014.03.004) PMID: [24704492](https://pubmed.ncbi.nlm.nih.gov/24704492/)
27. Re DB, Le Verche V, Yu C, Amoroso MW, Politi KA, et al. (2014) Necroptosis drives motor neuron death in models of both sporadic and familial ALS. *Neuron* 81: 1001–1008. doi: [10.1016/j.neuron.2014.01.011](https://doi.org/10.1016/j.neuron.2014.01.011) PMID: [24508385](https://pubmed.ncbi.nlm.nih.gov/24508385/)
28. Boillee S, Vande Velde C, Cleveland DW (2006) ALS: a disease of motor neurons and their nonneuronal neighbors. *Neuron* 52: 39–59. PMID: [17015226](https://pubmed.ncbi.nlm.nih.gov/17015226/)
29. Boillee S, Yamanaka K, Lobsiger CS, Copeland NG, Jenkins NA, et al. (2006) Onset and progression in inherited ALS determined by motor neurons and microglia. *Science* 312: 1389–1392. PMID: [16741123](https://pubmed.ncbi.nlm.nih.gov/16741123/)
30. Yamanaka K, Chun SJ, Boillee S, Fujimori-Tonou N, Yamashita H, et al. (2008) Astrocytes as determinants of disease progression in inherited amyotrophic lateral sclerosis. *Nat Neurosci* 11: 251–253. doi: [10.1038/nn2047](https://doi.org/10.1038/nn2047) PMID: [18246065](https://pubmed.ncbi.nlm.nih.gov/18246065/)
31. Kang SH, Li Y, Fukaya M, Lorenzini I, Cleveland DW, et al. (2013) Degeneration and impaired regeneration of gray matter oligodendrocytes in amyotrophic lateral sclerosis. *Nat Neurosci* 16: 571–579. doi: [10.1038/nn.3357](https://doi.org/10.1038/nn.3357) PMID: [23542689](https://pubmed.ncbi.nlm.nih.gov/23542689/)
32. Papadeas ST, Kraig SE, O'Banion C, Lepore AC, Maragakis NJ (2011) Astrocytes carrying the superoxide dismutase 1 (SOD1G93A) mutation induce wild-type motor neuron degeneration in vivo. *Proc Natl Acad Sci U S A* 108: 17803–17808. doi: [10.1073/pnas.1103141108](https://doi.org/10.1073/pnas.1103141108) PMID: [21969586](https://pubmed.ncbi.nlm.nih.gov/21969586/)
33. Di Giorgio FP, Boulting GL, Bobrowicz S, Eggan KC (2008) Human embryonic stem cell-derived motor neurons are sensitive to the toxic effect of glial cells carrying an ALS-causing mutation. *Cell Stem Cell* 3: 637–648. doi: [10.1016/j.stem.2008.09.017](https://doi.org/10.1016/j.stem.2008.09.017) PMID: [19041780](https://pubmed.ncbi.nlm.nih.gov/19041780/)
34. Marchetto MC, Muotri AR, Mu Y, Smith AM, Cezar GG, et al. (2008) Non-cell-autonomous effect of human SOD1 G37R astrocytes on motor neurons derived from human embryonic stem cells. *Cell Stem Cell* 3: 649–657. doi: [10.1016/j.stem.2008.10.001](https://doi.org/10.1016/j.stem.2008.10.001) PMID: [19041781](https://pubmed.ncbi.nlm.nih.gov/19041781/)
35. Donnelly CJ, Zhang PW, Pham JT, Heusler AR, Mistry NA, et al. (2013) RNA toxicity from the ALS/FTD C9ORF72 expansion is mitigated by antisense intervention. *Neuron* 80: 415–428. doi: [10.1016/j.neuron.2013.10.015](https://doi.org/10.1016/j.neuron.2013.10.015) PMID: [24139042](https://pubmed.ncbi.nlm.nih.gov/24139042/)
36. Su Z, Zhang Y, Gendron TF, Bauer PO, Chew J, et al. (2014) Discovery of a Biomarker and Lead Small Molecules to Target r(GGGGCC)-Associated Defects in c9FTD/ALS. *Neuron*.
37. Wray S, Self M, Lewis PA, Taanman JW, Ryan NS, et al. (2012) Creation of an open-access, mutation-defined fibroblast resource for neurological disease research. *PLoS One* 7: e43099. doi: [10.1371/journal.pone.0043099](https://doi.org/10.1371/journal.pone.0043099) PMID: [22952635](https://pubmed.ncbi.nlm.nih.gov/22952635/)
38. Hu BY, Zhang SC (2009) Differentiation of spinal motor neurons from pluripotent human stem cells. *Nat Protoc* 4: 1295–1304. doi: [10.1038/nprot.2009.127](https://doi.org/10.1038/nprot.2009.127) PMID: [19696748](https://pubmed.ncbi.nlm.nih.gov/19696748/)
39. Chambers SM, Fasano CA, Papapetrou EP, Tomishima M, Sadelain M, et al. (2009) Highly efficient neural conversion of human ES and iPSC cells by dual inhibition of SMAD signaling. *Nat Biotechnol* 27: 275–280. doi: [10.1038/nbt.1529](https://doi.org/10.1038/nbt.1529) PMID: [19252484](https://pubmed.ncbi.nlm.nih.gov/19252484/)
40. Roybon L, Lamas NJ, Garcia-Diaz A, Yang EJ, Sattler R, et al. (2013) Human stem cell-derived spinal cord astrocytes with defined mature or reactive phenotypes. *Cell Rep* 4: 1035–1048. doi: [10.1016/j.celrep.2013.06.021](https://doi.org/10.1016/j.celrep.2013.06.021) PMID: [23994478](https://pubmed.ncbi.nlm.nih.gov/23994478/)

41. Liu Y, Han SS, Wu Y, Tuohy TM, Xue H, et al. (2004) CD44 expression identifies astrocyte-restricted precursor cells. *Dev Biol* 276: 31–46. PMID: [15531362](#)
42. Donnelly CJ, Zhang PW, Pham JT, Haeusler AR, Mistry NA, et al. (2013) RNA toxicity from the ALS/FTD C9ORF72 expansion is mitigated by antisense intervention. *Neuron* 80: 415–428. doi: [10.1016/j.neuron.2013.10.015](#) PMID: [24139042](#)
43. Aasen T, Raya A, Barrero MJ, Garreta E, Consiglio A, et al. (2008) Efficient and rapid generation of induced pluripotent stem cells from human keratinocytes. *Nat Biotechnol* 26: 1276–1284. doi: [10.1038/nbt.1503](#) PMID: [18931654](#)
44. Loh YH, Agarwal S, Park IH, Urbach A, Huo H, et al. (2009) Generation of induced pluripotent stem cells from human blood. *Blood* 113: 5476–5479. doi: [10.1182/blood-2009-02-204800](#) PMID: [19299331](#)
45. Robinton DA, Daley GQ (2012) The promise of induced pluripotent stem cells in research and therapy. *Nature* 481: 295–305. doi: [10.1038/nature10761](#) PMID: [22258608](#)
46. Takahashi K, Yamanaka S (2006) Induction of pluripotent stem cells from mouse embryonic and adult fibroblast cultures by defined factors. *Cell* 126: 663–676. PMID: [16904174](#)
47. Zhou W, Freed CR (2009) Adenoviral gene delivery can reprogram human fibroblasts to induced pluripotent stem cells. *Stem Cells* 27: 2667–2674. doi: [10.1002/stem.201](#) PMID: [19697349](#)
48. Fusaki N, Ban H, Nishiyama A, Saeki K, Hasegawa M (2009) Efficient induction of transgene-free human pluripotent stem cells using a vector based on Sendai virus, an RNA virus that does not integrate into the host genome. *Proc Jpn Acad Ser B Phys Biol Sci* 85: 348–362. PMID: [19838014](#)
49. Woltjen K, Michael IP, Mohseni P, Desai R, Mileikovsky M, et al. (2009) piggyBac transposition reprograms fibroblasts to induced pluripotent stem cells. *Nature* 458: 766–770. doi: [10.1038/nature07863](#) PMID: [19252478](#)
50. Kaji K, Norrby K, Paca A, Mileikovsky M, Mohseni P, et al. (2009) Virus-free induction of pluripotency and subsequent excision of reprogramming factors. *Nature* 458: 771–775. doi: [10.1038/nature07864](#) PMID: [19252477](#)
51. Jia F, Wilson KD, Sun N, Gupta DM, Huang M, et al. (2010) A nonviral minicircle vector for deriving human iPS cells. *Nat Methods* 7: 197–199. doi: [10.1038/nmeth.1426](#) PMID: [20139967](#)
52. Yu J, Hu K, Smuga-Otto K, Tian S, Stewart R, et al. (2009) Human induced pluripotent stem cells free of vector and transgene sequences. *Science* 324: 797–801. doi: [10.1126/science.1172482](#) PMID: [19325077](#)
53. Warren L, Manos PD, Ahfeldt T, Loh YH, Li H, et al. (2010) Highly efficient reprogramming to pluripotency and directed differentiation of human cells with synthetic modified mRNA. *Cell Stem Cell* 7: 618–630. doi: [10.1016/j.stem.2010.08.012](#) PMID: [20888316](#)
54. Kim D, Kim CH, Moon JI, Chung YG, Chang MY, et al. (2009) Generation of human induced pluripotent stem cells by direct delivery of reprogramming proteins. *Cell Stem Cell* 4: 472–476. doi: [10.1016/j.stem.2009.05.005](#) PMID: [19481515](#)
55. Newman AM, Cooper JB (2010) Lab-specific gene expression signatures in pluripotent stem cells. *Cell Stem Cell* 7: 258–262. doi: [10.1016/j.stem.2010.06.016](#) PMID: [20682451](#)
56. Yang Y, Gozen O, Watkins A, Lorenzini I, Lepore A, et al. (2009) Presynaptic regulation of astroglial excitatory neurotransmitter transporter GLT1. *Neuron* 61: 880–894. doi: [10.1016/j.neuron.2009.02.010](#) PMID: [19323997](#)
57. Kola I, Landis J (2004) Can the pharmaceutical industry reduce attrition rates? *Nat Rev Drug Discov* 3: 711–715. PMID: [15286737](#)
58. Yang YM, Gupta SK, Kim KJ, Powers BE, Cerqueira A, et al. (2013) A Small Molecule Screen in Stem-Cell-Derived Motor Neurons Identifies a Kinase Inhibitor as a Candidate Therapeutic for ALS. *Cell Stem Cell* 12: 713–726. doi: [10.1016/j.stem.2013.04.003](#) PMID: [23602540](#)
59. Cleveland DW, Rothstein JD (2001) From Charcot to Lou Gehrig: deciphering selective motor neuron death in ALS. *Nat Rev Neurosci* 2: 806–819. PMID: [11715057](#)
60. Yamanaka S (2012) Induced pluripotent stem cells: past, present, and future. *Cell Stem Cell* 10: 678–684. doi: [10.1016/j.stem.2012.05.005](#) PMID: [22704507](#)
61. Grskovic M, Javaherian A, Strulovici B, Daley GQ (2011) Induced pluripotent stem cells—opportunities for disease modelling and drug discovery. *Nat Rev Drug Discov* 10: 915–929. doi: [10.1038/nrd3577](#) PMID: [22076509](#)
62. Rothstein JD, Van Kammen M, Levey AI, Martin LJ, Kuncl RW (1995) Selective loss of glial glutamate transporter GLT-1 in amyotrophic lateral sclerosis. *Ann Neurol* 38: 73–84. PMID: [7611729](#)
63. Corti S, Nizzardo M, Nardini M, Donadoni C, Salani S, et al. (2010) Systemic transplantation of c-kit+ cells exerts a therapeutic effect in a model of amyotrophic lateral sclerosis. *Hum Mol Genet* 19: 3782–3796. doi: [10.1093/hmg/ddq293](#) PMID: [20650960](#)
64. Ganel R, Ho T, Maragakis NJ, Jackson M, Steiner JP, et al. (2006) Selective up-regulation of the glial Na⁺-dependent glutamate transporter GLT1 by a neuroimmunophilin ligand results in neuroprotection. *Neurobiol Dis* 21: 556–567. PMID: [16274998](#)